Kyle I. Swanson, MD*
Paul A. Clark, PhD*
Ray R. Zhang, BS*‡
Irawati K. Kandela, PhD§
Mohammed Farhoud, MS¶
Jamey P. Weichert, PhD§¶||#
John S. Kuo, MD, PhD*‡#**

*Department of Neurological Surgery, ‡Cellular and Molecular Biology Training Program, ¶Department of Radiology, ||Department Medical Physics, and #Carbone Cancer Center, University of Wisconsin School of Medicine and Public Health, Madison, Wisconsin; §Cellectar Biosciences, Inc, Madison, Wisconsin; **Department of Surgery, National University of Singapore, Singapore

Correspondence:
John S. Kuo, MD, PhD, FAANS, FACS,
Department of Neurological Surgery,
University of Wisconsin School of
Medicine and Public Health,
Box 8660 Clinical Science Center,
600 Highland Ave,
Madison, WI 53792.
E-mail: j.kuo@neurosurgery.wisc.edu

Received, July 21, 2014.
Accepted, November 3, 2014.
Published Online, December 29, 2014.

A video abstract discussion by Drs Kuo and Weichert accompanies this article. Scan the QR code to view this video.

WHAT IS THIS BOX?
A QR Code is a matrix barcode readable by QR scanners, mobile phones with cameras, and smartphones. **The QR Code above links to Supplemental Digital Content from this article.**

Fluorescent Cancer-Selective Alkylphosphocholine Analogs for Intraoperative Glioma Detection

BACKGROUND: 5-Aminolevulinic acid (5-ALA)-induced tumor fluorescence aids brain tumor resections but is not approved for routine use in the United States. We developed and describe testing of 2 novel fluorescent, cancer-selective alkylphosphocholine analogs, CLR1501 (green) and CLR1502 (near infrared), in a proof-of-principle study for fluorescence-guided glioma surgery.

OBJECTIVE: To demonstrate that CLR1501 and CLR1502 are cancer cell-selective fluorescence agents in glioblastoma models and to compare tumor-to-normal brain (T:N) fluorescence ratios with 5-ALA.

METHODS: CLR1501, CLR1502, and 5-ALA were administered to mice with magnetic resonance imaging-verified orthotopic U251 glioblastoma multiforme- and glioblastoma stem cell-derived xenografts. Harvested brains were imaged with confocal microscopy (CLR1501), the IVIS Spectrum imaging system (CLR1501, CLR1502, and 5-ALA), or the Fluobeam near-infrared fluorescence imaging system (CLR1502). Imaging and quantitative analysis of T:N fluorescence ratios were performed.

RESULTS: Excitation/emission peaks are 500/517 nm for CLR1501 and 760/778 nm for CLR1502. The observed T:N ratio for CLR1502 (9.28 $\pm$ 1.08) was significantly higher ($P <$ .01) than for CLR1501 (3.51 $\pm$ 0.44 on confocal imaging; 7.23 $\pm$ 1.63 on IVIS imaging) and 5-ALA (4.81 $\pm$ 0.92). Near-infrared Fluobeam CLR1502 imaging in a mouse xenograft model demonstrated high- contrast tumor visualization compatible with surgical applications.

CONCLUSION: CLR1501 (green) and CLR1502 (near infrared) are novel tumor-selective fluorescent agents for discriminating tumor from normal brain. CLR1501 exhibits a tumor-to-brain fluorescence ratio similar to that of 5-ALA, whereas CLR1502 has a superior tumor-to-brain fluorescence ratio. This study demonstrates the potential use of CLR1501 and CLR1502 in fluorescence-guided tumor surgery.

KEY WORDS: Glioblastoma, Intraoperative imaging, Optical imaging, Tumor fluorescence

Neurosurgery 76:115–124, 2015 DOI: 10.1227/NEU.0000000000000622 www.neurosurgery-online.com

Evidence has accumulated that achieving a radiographic gross total resection (GTR) in high-grade gliomas (HGGs) improves overall survival. Two retrospective case-control series reported that GTR significantly improved overall survival from 8 to 13 months.[1,2] Despite evidence for a survival benefit, the overall rate of achieving GTR is relatively low. A literature meta-analysis found that the GTR rate was 62.3% (range, 33%-76%) for HGG.[3] Other reports suggest that even when tumor anatomy prevents safe GTR, maximizing extent of resection for HGG increases overall survival. Sanai et al[4] found a survival benefit even for a subtotal extent of resection down to 78%. The goal of increasing extent of resection to reduce tumor burden and to improve survival must be balanced against the higher risk of neurological deficits associated with more

ABBREVIATIONS: APC, alkylphosphocholine; **5-ALA,** 5-aminolevulinic acid; **GBM,** glioblastoma multiforme; **GSC,** glioblastoma stem cell; **GTR,** gross total resection; **HGG,** high-grade glioma; **PBS,** phosphate-buffered solution; **PpIX,** protoporphyrin IX; **T:N,** tumor to normal brain

Supplemental digital content is available for this article. Direct URL citations appear in the printed text and are provided in the HTML and PDF versions of this article on the journal's Web site (www.neurosurgery-online.com).

extensive resections, especially because postoperative neurological deficit is associated with diminished quality of life and survival.

Many innovative technologies are being developed to improve tumor visualization and to optimize strategies for maximal safe resection.[5] Innovations such as the operative microscope, intraoperative ultrasound, image-guided neuronavigation, and intraoperative magnetic resonance imaging (MRI) have been applied to improve tumor surgery.[6] Fluorescence agents for tumor detection or visualization are a promising new strategy to discriminate tumor from normal tissue and are being studied for maximizing safe surgical resection in multiple cancers, including bladder cancer, ovarian cancer, and brain tumors.[7-9]

5-Aminolevulinic acid (5-ALA) is currently approved in Europe for fluorescence-guided neurosurgery. 5-ALA is converted in tumors via the porphyrin synthesis pathway to protoporphyrin IX (PpIX; fluorescent excitation peak, 405 nm; emission peak, 635 nm).[10] Stummer et al[9,11-13] demonstrated that oral 5-ALA administration leads to relative accumulation of fluorescent PpIX in HGG, which discriminates tumor from normal brain in both rodents and humans. A phase IIIA trial comparing 5-ALA–guided HGG resection and standard microsurgery showed improved GTR (36% vs 65%) and better 6-month progression-free survival (41% vs 21%).[14] On the basis of the above study, 5-ALA use for HGG resection has been adopted internationally, but because the study was not powered adequately to address overall survival and did not involve US sites, 5-ALA is still not approved by the US Food and Drug Administration for routine use in America.

5-ALA–guided fluorescence of malignant gliomas provides unprecedented high positive predictive value and sensitivity.[15-19] Several methods are also being developed and tested to detect cases of low or variable tumor PpIX fluorescence signal, including intraoperative confocal microscopy[3,20-24] and intraoperative spectroscopy.[25-28] It is also unknown whether 5-ALA detects clinically significant subsets of cancer cells such as cancer stem cells. Therefore, many investigators are interested in developing new tumor visualization agents and technologies.

We recently reported preclinical and early human studies of cancer-targeted alkylphosphocholine (APC) analogs based on CLR1404 [18-(p-iodophenyl) octadecylphosphocholine] that display prolonged tumor-selective retention in many different cancers via testing of 55 different in vivo rodent and human cancer and cancer stem cell models.[29] Extensive in vitro and in vivo testing shows the inherent advantage of this new, broad-spectrum cancer-targeting platform: All APC analogs have identical tumor-specific uptake and persistence regardless of the added radioactive or fluorescence label.[29] Tumor-specific APC uptake, partly through the lipid raft-rich compartment of cancer cell membranes coupled with elimination from normal tissues over time, yields high tumor-specific discrimination and targeting for imaging and therapy.[29] Depending on the conjugated radiolabel, CLR1404 may be used for tumor-selective positron emission tomography imaging (^{124}I-CLR1404) or therapeutic radiation (^{131}I-CLR1404). Two fluorescent CLR1404 derivatives were also developed by substituting iodine with fluorescent moieties: CLR1501 (green) and CRL1502 (near infrared; Figure 1A). CLR1501 and CLR1502 also exhibit tumor selectivity in vitro and in vivo for human glioblastoma stem cell (GSC) lines and xenografts.[29] We envision and are developing the APC cancer-targeting platform for multiple steps in clinical cancer management: diagnostic cancer imaging, surgical tumor detection, and adjuvant cancer therapy. This study compares CLR1501 and CLR1502 with 5-ALA as tumor fluorescence agents and serves as a proof of principle for the potential use of fluorescent APC analogs in cancer surgery.

OBJECTIVES

This study aim to define the excitation/emission spectra of CLR1501 and CLR1502, to demonstrate that CLR1501 and CLR1502 fluorescence differentiates tumor and normal brain in mouse models of orthotopic U251 glioblastoma multiforme (GBM)- and GSC-derived xenografts, and to compare the tumor fluorescence of 5-ALA/PpIX with the 2 fluorescent APC analogs.

METHODS

Fluorescence Spectra Analysis

CLR1501 (18-[p-(4,4-difluoro-4-bora-3a,4a-diaza-s-indacene-8-yl)-phenyl]-octadecyl phosphocholine) and CLR1502 (1,3,3-trimethyl-2-[(E)-2-[(3E)-3-(2-[(2E)-1,3,3-trimethyl-2,3-dihydro-1H-indol-2-ylidene] ethylidene)-2-[4-(18-([2-(trimethylazaniumyl)ethyl phosphonato]oxy) octadecyl)phenyl]cyclohex-1-en-1-yl]ethenyl]-3H-indol-1-ium) were provided by Cellectar Biosciences, Inc (Madison, Wisconsin).[29] PpIX was purchased (P8293, Sigma-Aldrich, St. Louis, Missouri). CLR1501, CLR1502, and PpIX were diluted in ethanol at 40 μg/mL. Ethanol solvent was chosen to avoid the unwanted spectral shifts seen with dimethyl sulfoxide.[30] The agents were then analyzed in experimental triplicates with the Tecan Safire^2 microplate reader to obtain fluorescence excitation and emission spectra. The following spectra collection parameters were used: 1-nm increments, 10-nm bandwidth, 10 counts per wavelength, and gain of 90. Fluorescence spectra were normalized to peak values.

Orthotopic GBM Xenograft Model

All studies were performed under approved protocols by the University of Wisconsin-Madison Institutional Review Board and the Animal Care and Use Committee. Nonobese diabetic severe combined immunodeficient (NOD SCID) mice, U251 glioblastoma line, and our patient-derived 22T GBM and GSC lines were used. GSC lines (22CSC, 33CSC, 105CSC) were isolated and validated for multipotent differentiation and tumor initiation via orthotopic xenografts in our laboratory as previously reported.[31,32] In brief, cells passaged in vitro were enzymatically dissociated into single-cell suspensions, with between 2×10^5 and 1×10^6 cells suspended in 5 μL of phosphate-buffered solution (PBS). GSCs were stereotactically injected with a Hamilton syringe into the right striatum of anesthetized mice at a rate of 1 μL/min. Coordinates are referenced from bregma: 0 mm anteroposterior, +2.5 mm mediolateral, and −3.5 mm dorsoventral.[31-33] Either at onset of neurological

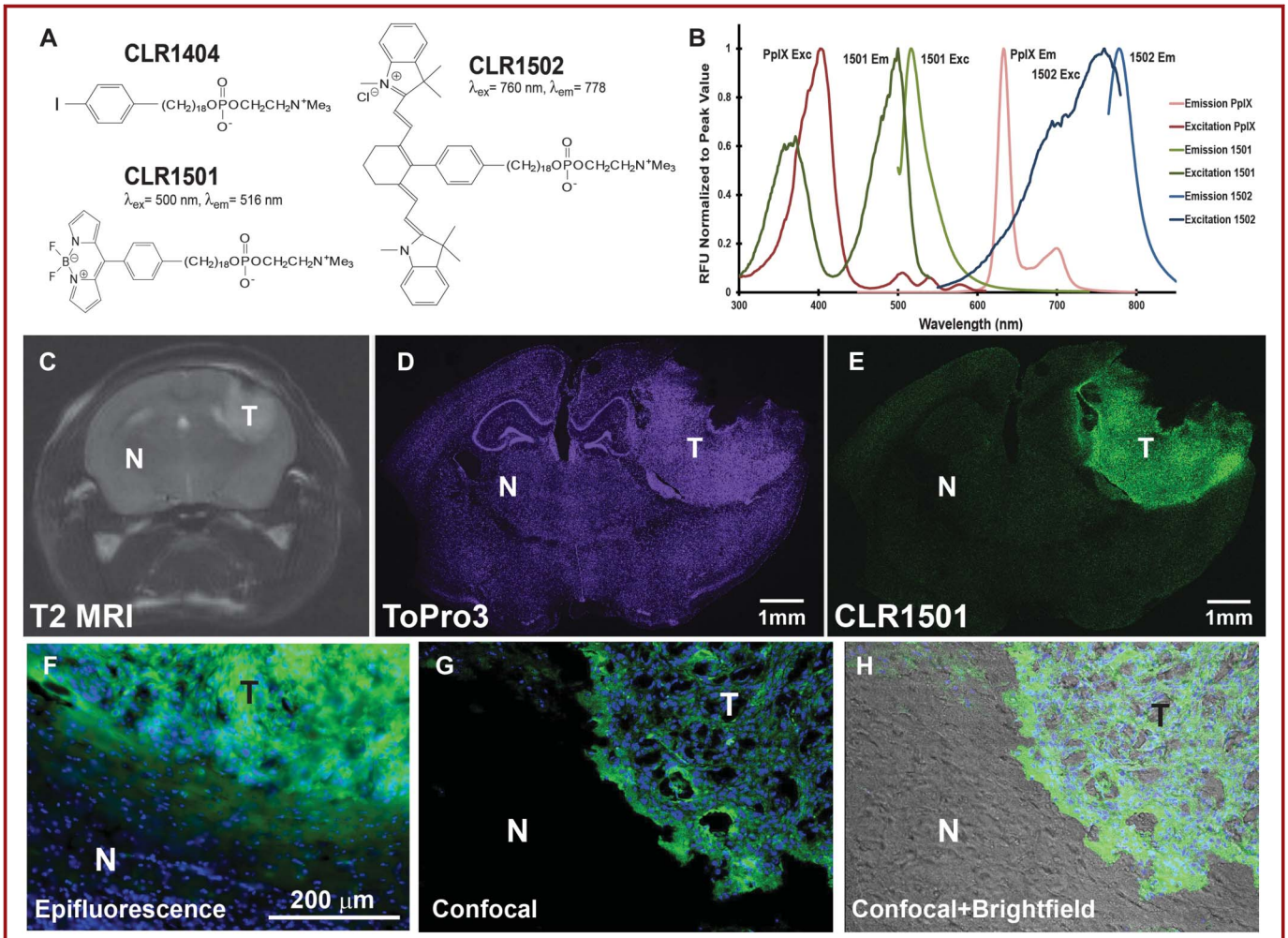

FIGURE 1. **A**, *chemical structures of APC analogs.* **B**, *fluorescence spectra: CLR1501 (excitation [Exc] peak, 500 nm; emission [Em] peak, 517 nm), CLR1502 (excitation peak, 760 nm; emission peak, 778 nm), and protoporphyrin IX (PpIX; excitation peak, 402 nm; emission peak, 633 nm).* **C** *through* **E**, *U251-derived orthotopic brain tumor verified by magnetic resonance imaging (MRI;* **C**, *T2-weighted) and labeled with CLR1501 (***E***) with ToPro3 nuclear counterstain (***D***).* **F** *through* **H**, *histological analysis of brain-tumor interface in 22T glioblastoma multiforme-derived orthotopic xenograft labeled with CLR1501 (green).* **F**, *epifluorescent visualization of xenograft-brain border with blue DAPI nuclear counterstain.* **G**, *confocal view of a xenograft labeled with CLR1501.* **H**, *confocal and bright-field view of xenograft and adjacent normal brain. N, normal brain; RFU, relative fluorescent units; T, tumor.*

symptoms or at 3 months, xenograft formation was verified with T2-weighted MRI using a 4.7-T horizontal-bore small-animal MRI scanner (Varian, Palo Alto, California).

Fluorescence Agents

CLR1501 and CLR1502 were formulated for intravenous injection as previously described.[29] 5-ALA purchased commercially (A3785, Sigma-Aldrich, St. Louis, Missouri) was dissolved in sterile saline. As recommended by the University of Wisconsin Animal Care committee, mice with documented orthotopic GSC or U251 xenografts received approximately 50 to 100 μL retro-orbital injections (equivalent to tail vein injections)[34,35] of CLR1501, CLR1502, 5-ALA, or a combination after isoflurane anesthesia induction: CLR1501 (16 mg/kg, 4 days before euthanasia), CLR1502 (2 mg/kg, 4 days before euthanasia), or 5-ALA (100 mg/kg, an average of 5 hours 45 minutes [range, 5 hours 10 minutes-6 hours 13 minutes] before euthanasia). After the elapsed time, mice were deeply anesthetized with xylazine/ketamine and then euthanized via perfusion fixation with 4% paraformaldehyde in PBS.

Confocal Imaging

Extracted brains were fixed in 4% paraformaldehyde overnight at 4°C and then placed in 30% sucrose in PBS at 4°C until saturation. Brains were then frozen in Tissue-Tek optimal-cutting-temperature compound (Sakura Finetek, Torrance, California) using an isopentane cryobath and stored at −80°C. The brains were cryosectioned at 100 μm, treated with 1 μmol/L ToPro3 iodide nuclear stain in PBS for 15 minutes (T3605, Molecular Probes, Eugene, Oregon), washed with PBS, and mounted with Prolong Gold antifade reagent (P36934, Molecular Probes).

Whole-brain sections were imaged with a Nikon A1RSi Confocal microscope (Nikon Instruments, Melville, New York) using ×10 magnification. CLR1501 fluorescence was imaged with a 488-nm excitation laser with a 525/550-nm emission filter, and ToPro3 fluorescence was imaged with a 640-nm excitation laser and 650-nm long-pass filter. NIS Elements Advanced software was used to measure the average CLR1501 fluorescence intensity of equivalent-sized regions of interest in tumors vs contralateral brain (determined by ToPro3 nuclear staining).

Ex Vivo Flow Cytometry

Tumor xenografts were microscopically dissected from mouse brains, with special care taken to minimize contamination with normal brain parenchyma. Xenografts were enzymatically dissociated with the use of Accutase for 15 minutes at 37°C, followed by mechanical trituration with a P200 pipette. The tissue slurry was filtered with a 40-μm cell strainer and resuspended in flow cytometry buffer (PBS + 1% goat serum). Cells were then washed multiple times and analyzed with the use of flow cytometry (FACScalibur, Becton Dickinson). The flow cytometer was corrected for background fluorescence (brain cells from animals that were not injected with CLR1501). Data were collected on 10000 cells using proper gating for CLR1501 (excitation/emission, 490/515 nm) and analyzed with WinMDI freeware (http://facs.scripps.edu/software.html). Live cells were gated using forward and side scatter. Proper gating is established to quantify positive vs negative fluorescent cells by comparison with isotype controls. Intensity is represented by relative fluorescent units or the geometric mean of resulting histograms.

IVIS Spectrum Imaging

Paraformaldehyde perfusion-fixed brains were bisected at the tumor injection site. The IVIS Spectrum system (Perkin-Elmer/Xenogen, Waltham, Massachusetts) was used to visualize the brains with measurements of average radiance ($p \cdot s^{-1} \cdot cm^{-2} \cdot sr^{-1}$) obtained from a standard-sized region of interest in the tumor compared with contralateral normal brain to calculate a ratio of average radiance. The following excitation/emission combinations were used: CLR1501, 500/540 nm; CLR1502, 745/800 nm; and 5-ALA, 430/640 nm. After IVIS imaging, the brains were embedded in paraffin, sectioned, stained with hematoxylin and eosin, and imaged with an EVOS XL Core bright-field microscope (Advanced Microscopy Group, Bothell, Washington) to verify tumor xenograft. It is important to note that because of technical constraints of the IVIS system, 5-ALA excitation was performed at 430 nm (range, 415-445 nm), not at the reported optimum of 402 nm.

Near-Infrared Imaging

CLR1502-injected mice were imaged with the Fluobeam 800 (Fluoptics, Grenoble, France), which is a hand-held imaging system designed for detecting in vivo near-infrared fluorescence (excitation laser wavelength of 780 nm and a charge-coupled device camera with filters to detect wavelengths >800 nm).[36-38] Imaging was conducted on mice before euthanasia and on the exposed or extracted brain after sacrifice. White-light photographs were also obtained. The brains were subsequently imaged with the IVIS Spectrum system as described above and then embedded in paraffin and processed for general histology. Some brains labeled with CLR1502 were also imaged with a Leica OH4 intraoperative microscope with a FL800 attachment (Leica Microsystems, Wetzlar, Germany), designed to image indocyanine green with an 800-nm excitation light and a near-infrared charge-coupled device camera with an 820- to 860-nm filter.[39,40]

Statistical Analysis

Statistical analyses were done with Microsoft Excel for Mac 2011 version 14.3.7. Comparisons of mean fluorescence ratio in tumor compared with contralateral normal brain (T:N) and T:N ratios between fluorescence agents were performed with a 1-tailed unpaired Student *t* test. All data with a value of $P < .05$ were considered significant. Numbers of experiments and mice used are indicated.

A total of 35 mice harboring xenografts (25 U251, 10GSC) were imaged on the IVIS system for CLR1501, CLR1502, or 5-ALA signal. A total of 9 mice (5 U251, 4 GSC-derived xenografts) were imaged on the Fluobeam near-infrared visualization system after CLR1502 injection.

RESULTS

CLR1501 and CLR1502 Spectra

CLR1501 has an excitation peak at 500 nm and emission peak at 517 nm in the visible green spectrum. CLR1502 has an excitation peak at 760 nm and emission peak at 778 nm in the near-infrared spectrum (Figure 1B). Similar to prior published data, the PpIX fluorescence spectra observed in our laboratory reveal a 402-nm excitation peak and a 633-nm emission peak.[10]

Confocal Imaging of CLR1501 Tumor Fluorescence

To avoid ethanol dehydration and extraction of CLR1501 and CLR1502 from tissues, frozen xenograft sections were used for imaging. Confocal imaging of frozen brain sections demonstrated a clear difference in CLR1501 fluorescence between tumor xenografts and contralateral normal brain (Figure 1C-1E, representative U251 xenograft). For U251 xenografts (n = 13), the observed average T:N fluorescence ratio was 3.51 ± 0.44 ($P < .001$). With 22T GBM-derived xenografts, representative magnified views of green fluorescent CLR1501 tumor label show the cellular margin between tumor and normal brain (Figure 1F-1H). For 22CSC xenografts (n = 2), the observed T:N fluorescence ratio was 5.84 ± 3.3, although the small sample size limits statistical impact.

CLR1501 Tumor Fluorescence by Flow Cytometry

After MRI-verified tumor growth, U251 glioblastoma xenografts from mice injected with CLR1501 (n = 4) were removed, analyzed by ex vivo flow cytometry, and compared with normal contralateral brain. U251 xenografts revealed a mean T:N ratio of 14.8 ± 7.34 ($P = .07$; Figure 2A).

IVIS Tumor Fluorescence Imaging: CLR1501 vs 5-ALA

For all U251 glioblastoma xenografts from mice injected with CLR1501 (n = 18) and imaged with IVIS (excitation/emission, 500/540 nm), the mean T:N fluorescence ratio was 7.23 ± 1.63. This was significantly higher than the observed mean T:N ratio of 0.87 ± 0.07 ($P < .001$) of the negative controls: U251

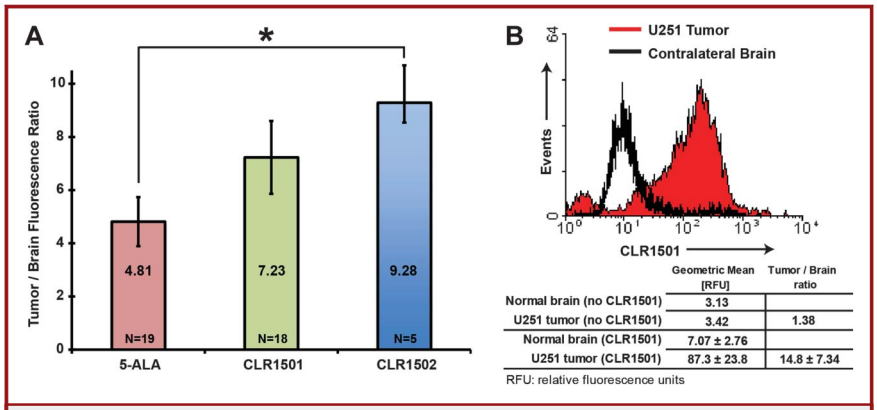

	Geometric Mean [RFU]	Tumor / Brain ratio
Normal brain (no CLR1501)	3.13	
U251 tumor (no CLR1501)	3.42	1.38
Normal brain (CLR1501)	7.07 ± 2.76	
U251 tumor (CLR1501)	87.3 ± 23.8	14.8 ± 7.34

RFU: relative fluorescence units

FIGURE 2. **A**, *CLR1501 tumor-to-brain fluorescence ratios for U251-derived orthotopic xenograft.* **B**, *flow cytometry of CLR1501$^+$ cells from U251-derived orthotopic xenograft compared with normal brain. 5-ALA, 5-aminolevulinic acid; RFU, relative fluorescent units.*

xenografts not exposed to CLR1501 (n = 7) that were imaged at the same settings.

The observed mean T:N fluorescence ratio was 4.81 ± 0.92 for all U251 xenografts from mice treated with 5-ALA (n = 19) and imaged with IVIS (excitation/emission, 430/640 nm). This was significantly higher than the observed mean T:N ratio of 1.14:0.19 ($P < .001$) of the negative controls, U251 xenografts not treated with 5-ALA (n = 6) and imaged at the same settings. Overall, CLR1501-treated mice had a higher mean T:N fluorescence ratio than 5-ALA–treated mice, but the difference was not statistically significant (7.23 ± 1.63 vs 4.81 ± 0.92; $P = .08$).

Direct comparison of CLR1501 with 5-ALA was performed in 15 mice harboring U251 xenografts that were cotreated with both agents. The observed mean T:N fluorescence ratio was higher for CLR1501 (6.88 ± 1.57) than 5-ALA (4.00 ± 0.97), but the difference was not significant ($P = .07$).

The measured average radiance of U251 tumors labeled with CLR1501 ($3.15 \times 10 \pm 5.66 \times 10^7$ p·s^{-1}·cm^{-2}·sr^{-1}) was higher than tumors labeled with 5-ALA ($2.17 \times 10 \pm 3.52 \times 10^6$ p·s^{-1}·cm^{-2}·sr^{-1}), but this was due in part to the background autofluorescence also being higher at the settings used for imaging CLR1501 ($1.67 \times 10 \pm 3.03 \times 10^6$ p·s^{-1}·cm^{-2}·sr^{-1}) than for 5-ALA imaging ($2.93 \times 10 \pm 4.71 \times 10^5$ p·s^{-1}·cm^{-2}·sr^{-1}).

For 105CSC xenografts, the mean T:N fluorescence ratio trended higher for CLR1501 (12.04 ± 3.64; n = 2) than for 5-ALA (6.52 ± 1.63; n = 3), but these data did not reach significance, partly because of the small sample sizes ($P = .17$). It is important to note that as a result of technical constraints of the IVIS system, 5-ALA excitation was performed at 430 nm (range, 415-445 nm), not at the reported optimal 402-nm wavelength.

IVIS Fluorescence Imaging: CLR1502 vs 5-ALA and CLR1501

For U251 glioblastoma xenografts in mice treated with CLR1502 (n = 5) and imaged with IVIS (excitation/emission, 745/800 nm), the mean T:N fluorescence ratio was 9.28 ± 1.08. This is significantly higher than the mean T:N ratio of 1.03 ± 0.01 ($P < .001$) for the negative controls: U251 xenografts in mice not injected with CLR1502 (n = 20) imaged at the same settings.

For U251 xenografts, the mean T:N ratio was significantly higher for CLR1502 (9.28 ± 1.08) than for 5-ALA (4.81 ± 0.92; $P < .01$). Although the mean T:N ratio was higher for CLR1502 (9.28 ± 1.08) than for CLR1501 (7.23 ± 1.63), the difference was not significant ($P = .13$; Figure 2B).

For 33CSC xenografts and 105CSC xenografts, the sample size was too small to statistically compare CLR1502 with 5-ALA, but significant CLR1502 tumor fluorescence was observed in xenografts derived from both CSC lines. For 33CSC xenografts, the mean T:N ratio for CLR1502 (n = 2) was 5.47 ± 3.12. This compares with the 33CSC mouse xenografts (n = 1) treated with 5-ALA with a T:N ratio of 6.20. For 105CSC xenografts, the mean T:N ratio for CLR1502 (n = 3) was 13.31 ± 3.42, which was not statistically significant from the mean T:N ratio for 5-ALA (n = 3), 6.52 ± 1.63 ($P = .09$).

The measured average radiance of U251 tumors labeled with CLR1502 is $6.92 \times 10 \pm 7.30 \times 10^7$ p·s^{-1}·cm^{-2}·sr^{-1}, higher than both CLR1501- and 5-ALA–labeled tumors, but the background autofluorescence measured at the CLR1502 imaging settings is low ($4.45 \times 10 \pm 3.40 \times 10^5$ p·s^{-1}·cm^{-2}·sr^{-1}), similar to the autofluorescence at the 5-ALA settings and less than the autofluorescence at the CLR1501 settings. As noted, 5-ALA excitation was performed from 415 to 445 nm, not at the reported optimal 402 nm, because of IVIS system technical constraints.

CLR1502 Visualization With Fluobeam and the Leica OH4 Microscope

Near-infrared imaging of CLR1502 fluorescence with the Fluobeam device provided excellent macroscopic tumor

delineation from normal brain (Figure 3) for all tested GBM/GSC-derived xenografts (U251, 22CSC, 33CSC, 105CSC). Resected tissues with CLR1502 near-infrared fluorescence were confirmed as tumor on hematoxylin and eosin sections (Figure 3E), and the adjacent minimally fluorescent tissue was confirmed as nontumor brain (Figure 3F). Under nonoptimized conditions, distinct near-infrared tumor fluorescence was also detectable in CLR1502-labeled U251 xenografts (n = 2) with a standard Leica OH4 operative microscope with the FL800 attachment (Figure 4). Near-infrared imaging of CLR1502 tumor fluorescence successfully localized tumor through intact skin and skull in a live mouse and provided excellent tumor delineation on tumor resection after euthanasia, serving as proof of principle for CLR1502 fluorescence-guided tumor surgery (see the **Video**, **Supplemental Digital Content**, http://links.lww.com/NEU/A703, which shows

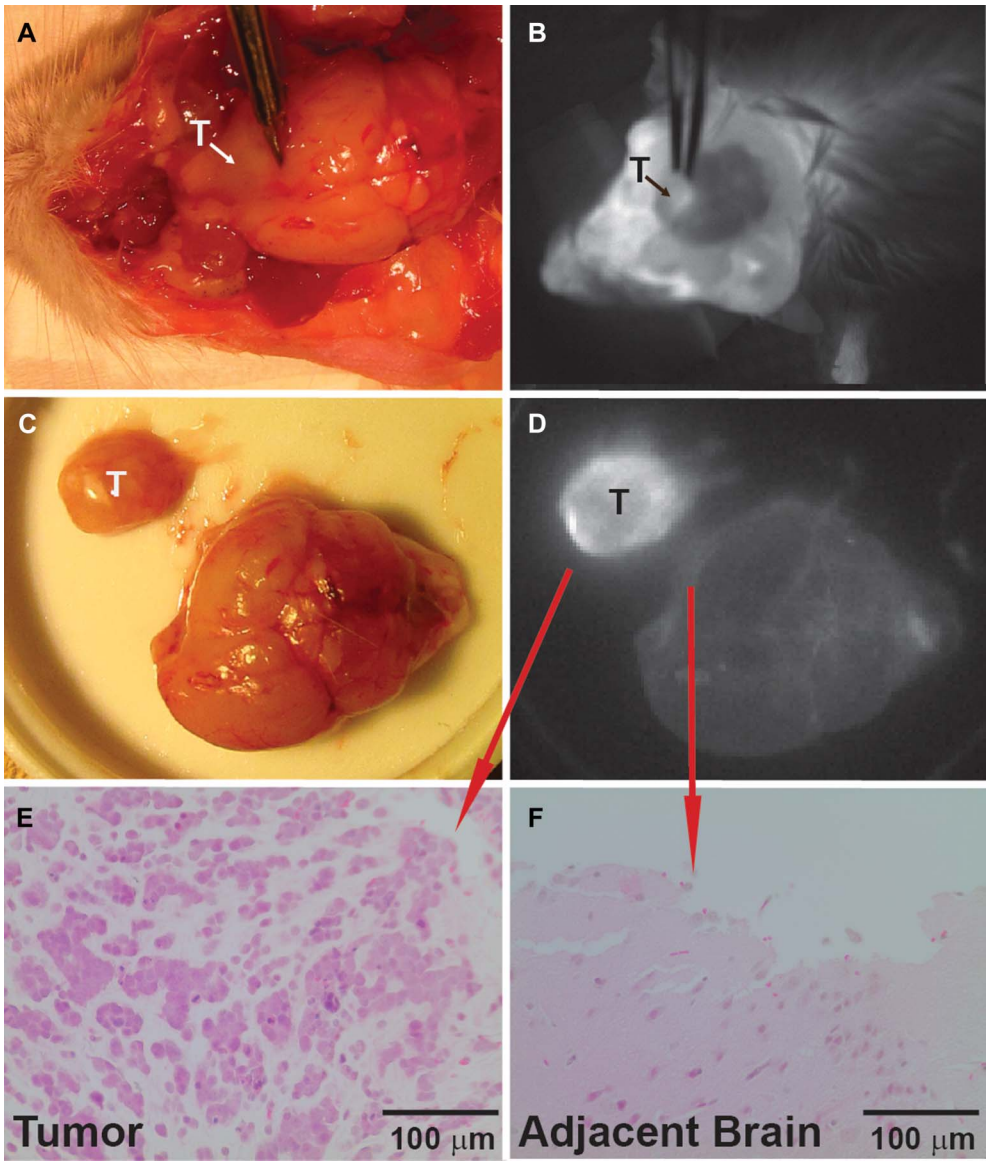

FIGURE 3. **A** *and* **B**, *CLR1502 fluorescence of 22CSC-derived orthotopic xenograft (***B***) compared with visible light (***A***).* **C** *and* **D**, *CLR1502 fluorescence of 22CSC-derived xenograft demonstrating excellent macroscopic tumor delineation from normal brain (***D***) compared with visible light (***C***).* **E** *and* **F**, *verification of tumor (T;* **E***) and normal brain (N;* **F***) by histology (hematoxylin and eosin).*

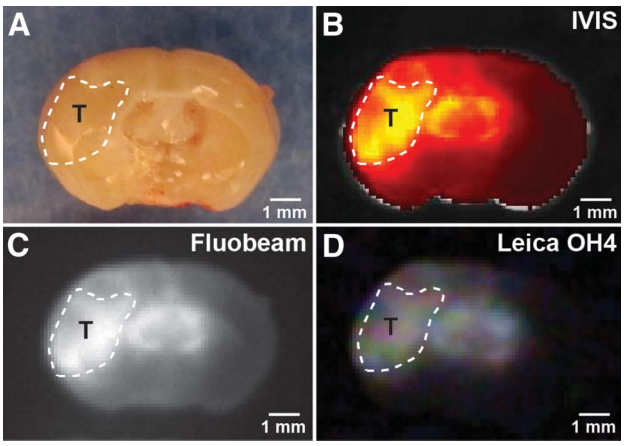

FIGURE 4. *Comparison of nonoptimized CLR1502 tumor fluorescent visualization using visible light (A), preclinical IVIS Spectrum (B), Fluobeam (C), and clinical Leica OH4 (D) systems. T, tumor xenograft (outlined by dotted line).*

CLR1502 fluorescence visualization of U251-derived xenograft in mouse).

DISCUSSION

Using multiple imaging modalities and primarily the U251 GBM model (and multiple GSC-derived xenografts), this study demonstrated that CLR1501 and CLR1502 provide excellent fluorescence discrimination of tumor from adjacent normal brain. CLR1501 provides fluorescence in the green spectrum (excitation/emission, 500/517 nm) and shows good tumor-to-brain distinction using confocal microscopy, ex vivo flow cytometry, and IVIS Spectrum imaging. CLR1502 provides fluorescence in the near-infrared spectrum (excitation/emission, 760/778 nm) and shows very high tumor-to-brain distinction using all 3 modalities of IVIS Spectrum imaging, Fluobeam detection, and commercially available operative microscopes with appropriate fluorescence detection attachments. The capability of already approved and available commercial imaging systems to visualize these tumor fluorescence agents would accelerate translation to clinical use.

Comparison of CLR1501 and CLR1502 with 5-ALA is important because 5-ALA is the current standard for fluorescence-guided neurosurgery. With the use of IVIS Spectrum imaging of mice harboring U251 GBM xenografts, direct comparison of CLR1501 and CLR1502 with 5-ALA showed that the mean CLR1501 T:N fluorescence ratio is comparable to the 5-ALA ratio, whereas the mean CLR1502 T:N fluorescence ratio was significantly higher than the 5-ALA ratio. Additionally, a near-infrared agent like CLR1502 is attractive for fluorescence-guided resection because of the decreased tissue absorption of light and relative low tissue autofluorescence at the near-infrared spectrum. Therefore, use of near-infrared fluorescence will help minimize the loss of signal caused by bleeding during resections.[41,42]

Limitations

Still, a current limitation of using near infrared fluorescence agents in surgery is that tumor is visualized on a separate monitor in a darkened operating theater, and surgeons cannot simultaneously visualize the resection field and instruments directly, as in 5-ALA–guided surgeries under blue light. Conceptual solutions are being developed such as projecting a "heads-up" display of the near-infrared fluorescence image to 1 microscope eyepiece or other methods to enable surgeons to simultaneously see overlapping bright-field and near-infrared images in the operative microsurgical view. Development of the optimal technologies for practical surgical use of these fluorescent APC analogs is still in progress.

We also acknowledge the inherent limitations in this proof-of-principle study resulting from the use of mouse tumor xenograft models derived from implanting human GBM and GSC lines and nonoptimized dosing, administration, and detection parameters. Questions relating to optimal APC dose, timing of administration, tumor uptake, persistence of tumor fluorescence, and optimal time window for surgical visualization will need to be answered through clinical trials with human cancer patients. We reported that preclinical and human data obtained with multiple radioiodinated APC analogs with regard to safety, tumor selective uptake, and retention were nearly identical, likely as a result of the identical molecular composition of the parental CLR1404 analog.[29,43] Studies with multiple fluorescent (CLR1501, CLR1502) and other APC analogs are underway to directly establish the temporal profile and to discover details of their interactions with tumor cells, tumor-brain and blood-brain barriers, especially to determine practical surgical timing, dose, visualization, and other parameters.

Clinical Potential

In preparation for clinical trials, the federally mandated safety testing of these novel fluorescent APC analogs was just completed. No overt toxicity was noted with either CLR1501 or CLR1502 during multiple preclinical studies. The parent APC analog CLR1404 (CLR1501 and CLR1502 are fluorescent analogs) has undergone extensive animal and human safety testing. Results from the multi-institutional phase I trial of therapeutic ^{131}I-CLR1404 in advanced cancer patients were recently reported.[43] Radioiodinated APC analogs are currently in phase II clinical trials, and upcoming clinical trials in human tumors are planned for these promising tumor-selective fluorescence agents.

In addition to fluorescence tumor differentiation with CLR1501 and CLR1502, we hypothesize that coinjection with the related radioiodinated ^{124}I-CLR1404 analog (for preoperative positron emission tomography/computed tomography tumor imaging) would correlate preoperative localization of tumor with intraoperative tumor fluorescence label and potentially improve extent of resection. Postoperative positron emission tomography/computed tomography imaging may also provide precise, cellular definition of any residual tumor cells (eg, define extent of resection).[29] Then, follow-up adjuvant therapies that include

administration of therapeutic ^{131}I-CLR1404 would target residual or unresectable tumor cells remaining after maximal surgery.[29] Clinical trials to optimize imaging dose and timing parameters are underway for the radioiodinated APC analogs and will prove useful for optimizing fluorescent APC surgical clinical trials to achieve the multimodality strategy of using APC diagnostics and therapeutics against cancer.

CONCLUSION

CLR1501 (green; excitation/emission, 500/517 nm) and CLR1502 (near-infrared; excitation/emission, 760/778 nm) are novel fluorescent derivatives of tumor-targeting APC analogs.[29] Their tumor fluorescence is readily detected with current clinically used, readily available indocyanine green fluorescence microscopes. CLR1501 and CLR1502 provided excellent tumor-to-normal brain fluorescence discrimination with in vivo GBM- and GSC-derived xenograft mouse models. Compared with 5-ALA, CLR1502 showed a superior tumor-to-brain fluorescence ratio. This study demonstrates the practical and promising potential of CLR1501 and CLR1502 analogs for use in fluorescence-guided tumor surgery.

Disclosures

These National Institutes of Health grants provided partial support: R21CA161704 (Drs Clark and Kuo), MSTP training fellowship (University of Wisconsin MSTP T32GM008692 to R.R. Zhang), R01CA158800 (Drs Kuo and Weichert), and R01NS075995 (Dr Kuo). We appreciate unrestricted support from the Headrush Brain Tumor Research Professorship and Roger Loff Memorial Fund for GBM Research (Dr Kuo). General funding was provided by University of Wisconsin Carbone Cancer Center, Wisconsin Partnership Program core grant support of the Center for Stem Cell and Regenerative Medicine, University of Wisconsin (Graduate School, Departments of Radiology, Medical Physics, Human Oncology, Neurological Surgery, Wisconsin Alumni Research Foundation, and Wisconsin Institutes of Discovery). Pilot grants and small-animal imaging were supported by the University of Wisconsin Carbone Cancer Center National Cancer Institute Support grant (P30 CA014520) and Waisman Center core grant from the National Institute of Child Health and Human Development (P30 HD03352). Dr Weichert is a cofounder of Cellectar Biosciences Inc, which owns licensing and patent rights to CLR1501, CLR1502, and related agents described in this article. The other authors have no personal, financial, or institutional interest in any of the drugs, materials, or devices described in this article.

REFERENCES

1. Lacroix M, Abi-Said D, Fourney DR, et al. A multivariate analysis of 416 patients with glioblastoma multiforme: prognosis, extent of resection, and survival. *J Neurosurg.* 2001;95(2):190-198.
2. McGirt MJ, Chaichana KL, Gathinji M, et al. Independent association of extent of resection with survival in patients with malignant brain astrocytoma. *J Neurosurg.* 2009;110(1):156-162.
3. Sanai N, Snyder LA, Honea NJ, et al. Intraoperative confocal microscopy in the visualization of 5-aminolevulinic acid fluorescence in low-grade gliomas. *J Neurosurg.* 2011;115(4):740-748.
4. Sanai N, Polley MY, McDermott MW, Parsa AT, Berger MS. An extent of resection threshold for newly diagnosed glioblastomas. *J Neurosurg.* 2011;115(1):3-8.
5. Liu JT, Meza D, Sanai N. Trends in fluorescence image-guided surgery for gliomas. *Neurosurgery*. 2014;75(1):61-71.
6. Kubben PL, ter Meulen KJ, Schijns OE, ter Laak-Poort MP, van Overbeeke JJ, van Santbrink H. Intraoperative MRI-guided resection of glioblastoma multiforme: a systematic review. *Lancet Oncol.* 2011;12(11):1062-1070.
7. Inoue K, Fukuhara H, Shimamoto T, et al. Comparison between intravesical and oral administration of 5-aminolevulinic acid in the clinical benefit of photodynamic diagnosis for nonmuscle invasive bladder cancer. *Cancer*. 2012;118(4):1062-1074.
8. van Dam GM, Themelis G, Crane LM, et al. Intraoperative tumor-specific fluorescence imaging in ovarian cancer by folate receptor-alpha targeting: first in-human results. *Nat Med.* 2011;17(10):1315-1319.
9. Stummer W, Stocker S, Wagner S, et al. Intraoperative detection of malignant gliomas by 5-aminolevulinic acid-induced porphyrin fluorescence. *Neurosurgery*. 1998;42(3):518-525; discussion 525-526.
10. Shepherd M, Dailey HA. A continuous fluorimetric assay for protoporphyrinogen oxidase by monitoring porphyrin accumulation. *Anal Biochem.* 2005;344(1):115-121.
11. Stummer W, Novotny A, Stepp H, Goetz C, Bise K, Reulen HJ. Fluorescence-guided resection of glioblastoma multiforme by using 5-aminolevulinic acid-induced porphyrins: a prospective study in 52 consecutive patients. *J Neurosurg.* 2000;93(6):1003-1013.
12. Stummer W, Stepp H, Moller G, Ehrhardt A, Leonhard M, Reulen HJ. Technical principles for protoporphyrin-IX-fluorescence guided microsurgical resection of malignant glioma tissue. *Acta Neurochir (Wien).* 1998;140(10):995-1000.
13. Stummer W, Stocker S, Novotny A, et al. In vitro and in vivo porphyrin accumulation by C6 glioma cells after exposure to 5-aminolevulinic acid. *J Photochem Photobiol B.* 1998;45(2-3):160-169.
14. Stummer W, Pichlmeier U, Meinel T, et al. Fluorescence-guided surgery with 5-aminolevulinic acid for resection of malignant glioma: a randomised controlled multicentre phase III trial. *Lancet Oncol.* 2006;7(5):392-401.
15. Diez Valle R, Tejada Solis S, Idoate Gastearena MA, Garcia de Eulate R, Dominguez Echavarri P, Aristu Mendiroz J. Surgery guided by 5-aminolevulinic fluorescence in glioblastoma: volumetric analysis of extent of resection in single-center experience. *J Neurooncol.* 2011;102(1):105-113.
16. Hefti M, von Campe G, Moschopulos M, Siegner A, Looser H, Landolt H. 5-Aminolevulinic acid induced protoporphyrin IX fluorescence in high-grade glioma surgery: a one-year experience at a single institution. *Swiss Med Wkly.* 2008;138(11-12):180-185.
17. Roberts DW, Valdes PA, Harris BT, et al. Coregistered fluorescence-enhanced tumor resection of malignant glioma: relationships between delta-aminolevulinic acid-induced protoporphyrin IX fluorescence, magnetic resonance imaging enhancement, and neuropathological parameters: clinical article. *J Neurosurg.* 2011;114(3):595-603.
18. Panciani PP, Fontanella M, Schatlo B, et al. Fluorescence and image guided resection in high grade glioma. *Clin Neurol Neurosurg.* 2012;114(1):37-41.
19. Nabavi A, Thurm H, Zountsas B, et al. Five-aminolevulinic acid for fluorescence-guided resection of recurrent malignant gliomas: a phase II study. *Neurosurgery*. 2009;65(6):1070-1076; discussion 1076-1077.
20. Eschbacher J, Martirosyan NL, Nakaji P, et al. In vivo intraoperative confocal microscopy for real-time histopathological imaging of brain tumors. *J Neurosurg.* 2012;116(4):854-860.
21. Nikolay M, Cavalcanti D, Eschbacher J, et al. Use of indocyanine green near-infrared laser confocal endomicroscopy in vivo: potential to intraoperatively detect the boundary of infiltrative tumor. *Neurosurgery*. 2011;115(6):1131-1138.
22. Sanai N, Eschbacher J, Hattendorf G, et al. Intraoperative confocal microscopy for brain tumors: a feasibility analysis in humans. *Neurosurgery*. 2011;68(2 suppl operative):282-290; discussion 290.
23. Sankar T, Delaney PM, Ryan RW, et al. Miniaturized handheld confocal microscopy for neurosurgery: results in an experimental glioblastoma model. *Neurosurgery*. 2010;66(2):410-417; discussion 417-418.
24. Schlosser HG, Suess O, Vajkoczy P, van Landeghem FK, Zeitz M, Bojarski C. Confocal neurolasermicroscopy in human brain: perspectives for neurosurgery on a cellular level (including additional comments to this article). *Cent Eur Neurosurg.* 2010;71(1):13-19.
25. Kim A, Khurana M, Moriyama Y, Wilson BC. Quantification of in vivo fluorescence decoupled from the effects of tissue optical properties using fiber-optic spectroscopy measurements. *J Biomed Opt.* 2010;15(6):067006.
26. Valdes PA, Kim A, Brantsch M, et al. Delta-aminolevulinic acid-induced protoporphyrin IX concentration correlates with histopathologic markers of malignancy in human gliomas: the need for quantitative fluorescence-guided

resection to identify regions of increasing malignancy. *Neuro Oncol.* 2011;13(8):846-856.
27. Valdes PA, Leblond F, Jacobs VL, Wilson BC, Paulsen KD, Roberts DW. Quantitative, spectrally-resolved intraoperative fluorescence imaging. *Sci Rep.* 2012;2:798.
28. Valdes PA, Leblond F, Kim A, et al. Quantitative fluorescence in intracranial tumor: implications for ALA-induced PpIX as an intraoperative biomarker. *J Neurosurg.* 2011;115(1):11-17.
29. Weichert JP, Clark PA, Kandela IK, et al. Alkylphosphocholine analogs for broad-spectrum cancer imaging and therapy. *Sci Transl Med.* 2014;6(240):240ra275.
30. Pretsch E, Bühlmann P, Badertscher M. *Solvent Corrections*. Berlin: Springer; 2009:401-420.
31. Clark PA, Iida M, Treisman DM, et al. Activation of multiple ERBB family receptors mediates glioblastoma cancer stem-like cell resistance to EGFR-targeted inhibition. *Neoplasia.* 2012;14(5):420-428.
32. Zorniak M, Clark PA, Leeper HE, et al. Differential expression of 2′,3′-cyclic-nucleotide 3′-phosphodiesterase and neural lineage markers correlate with glioblastoma xenograft infiltration and patient survival. *Clin Cancer Res.* 2012;18(13):3628-3636.
33. Galli R, Binda E, Orfanelli U, et al. Isolation and characterization of tumorigenic, stem-like neural precursors from human glioblastoma. *Cancer Res.* 2004;64(19):7011-7021.
34. Nanni C, Pettinato C, Ambrosini V, et al. Retro-orbital injection is an effective route for radiopharmaceutical administration in mice during small-animal PET studies. *Nucl Med Commun.* 2007;28(7):547-553.
35. Yardeni T, Eckhaus M, Morris HD, Huizing M, Hoogstraten-Miller S. Retro-orbital injections in mice. *Lab Anim (NY).* 2011;40(5):155-160.
36. Keramidas M, Josserand V, Righini CA, Wenk C, Faure C, Coll JL. Intraoperative near-infrared image-guided surgery for peritoneal carcinomatosis in a preclinical experimental model. *Br J Surg.* 2010;97(5):737-743.
37. Mery E, Jouve E, Guillermet S, et al. Intraoperative fluorescence imaging of peritoneal dissemination of ovarian carcinomas: a preclinical study. *Gynecol Oncol.* 2011;122(1):155-162.
38. Wenk CH, Ponce F, Guillermet S, et al. Near-infrared optical guided surgery of highly infiltrative fibrosarcomas in cats using an anti-alphavss3 integrin molecular probe. *Cancer Lett.* 2013;334(2):188-195.
39. Gioux S, Choi HS, Frangioni JV. Image-guided surgery using invisible near-infrared light: fundamentals of clinical translation. *Mol Imaging.* 2010;9(5):237-255.
40. Raabe A, Nakaji P, Beck J, et al. Prospective evaluation of surgical microscope-integrated intraoperative near-infrared indocyanine green videoangiography during aneurysm surgery. *J Neurosurg.* 2005;103(6):982-989.
41. Frangioni JV. In vivo near-infrared fluorescence imaging. *Curr Opin Chem Biol.* 2003;7(5):626-634.
42. Gibbs SL. Near infrared fluorescence for image-guided surgery. *Quant Imaging Med Surg.* 2012;2(3):177-187.
43. Grudzinski J, Titz B, Kozak K, et al. A phase 1 study of ^{131}I-CLR1404 in patients with relapsed or refractory advanced solid tumors: dosimetry, biodistribution, pharmacokinetics, and safety. *PLoS One.* 9(11):e111652.

Supplemental digital content *is available for this article. Direct URL citations appear in the printed text and are provided in the HTML and PDF versions of this article on the journal's Web site (www.neurosurgery-online.com).*

Acknowledgments

The authors thank Anatoly Pinchuk, PhD, for APC analog synthesis and analysis and Marc Longino, PhD, for formulating agents for in vivo injection.

COMMENTS

Alkylphosphocholine (APC) analogs are being explored for targeting a variety of tumors. They appear to have an affinity to cancer cell membranes where, unlike in normal cells, they cannot be metabolized. When coupled to radioactive iodine or to fluorescent moieties, this unique facility of APC analogs might be useful for treating or for intraoperative detection of tumors. Because the marginal tissue of malignant gliomas is difficult to detect in neurosurgical procedures, the authors explore 2 APC analogs coupled to fluorescent moieties for identifying experimental brain tumors and tumor stem cell-derived brain tumors in vivo.

One of the APC analogs has fluorescence in the visible (green) range (CLR1501, 517 nm); the other (CLR1502), in the infrared range, invisible to the human eye (778 nm). Using different methods (fluorescence-activated cell sorting, spectrometrical imaging, confocal imaging, and a standard surgical microscope equipped for indocyanine green angiography), the authors detect and visualize the 2 APC analogs. Using spectrometrical methods, they compare the fluorescence ratio between normal brain and tumor tissue with the fluorescence ratio found when they visualized their in vivo tumors with 5-aminolevulinic acid-derived protoporphyrin IX fluorescence, the latter having come into widespread clinical use. They report high tumor:normal fluorescence ratios for both compounds in their U251 tumor model, which was similar to 5-aminolevulinic acid-derived protoporphyrin IX fluorescence.

The authors are the first to explore these compounds for visualizing malignant glioma cells in the brain. Thus, this work is original and bears interest. However, many questions remain unanswered from this report. The images selected for demonstrating differential uptake suggest that the tumors have a wide margin of unspecific fluorescence. Possibly a strong time dependence is to be expected as the fluorophores circulate with blood, and selectivity will vary over time after intravenous application. It will be interesting to see how this promising technique develops in the future.

Walter Stummer
Münster, Germany

The authors discuss a new class of fluorescent alkylphosphocholine analogs that are being studied for intraoperative detection of malignant gliomas. The authors have published a prior report describing these analogs radiolabeled with ^{124}I or ^{131}I with labeling of human cancer cell lines (including glioma stem-like cells) in vitro and in vivo for positron emission tomography imaging and targeted radiotherapy.[1] These analogs have been modified now in this article with replacement of the radiolabeled iodine for fluorescent markers. CLR1501 is green with excitation at 500 nm, and CLR1502 is excited by near-infrared light >700 nm. The authors are able to demonstrate fluorescence in vivo with human orthotopic glioblastoma multiforme xenografts implanted in rodents. The use of compound 1502 results in better visualization of tumor fluorescence and less tissue autofluorescence, which may ultimately permit better visualization of malignant gliomas with near-infrared excitation.

Further testing of these agents is warranted to determine their positive predictive value of tissue fluorescence and malignant glioma tissue in patients. How effectively the analogs can cross the blood-brain barrier, be taken up by the tumor bulk, and infiltrate malignant glioma cells remains to be seen. The authors provide a nice contribution to the rapidly evolving field of fluorescence-guided surgery of malignant gliomas.

Costas G. Hadjipanayis
Atlanta, Georgia

1. Weichert JP, Clark PA, Kandela IK, et al. Alkylphosphocholine analogs for broad-spectrum cancer imaging and therapy. *Sci Transl Med.* 2014;6(240):240ra75.

The authors present their experience with the preclinical development of alkylphosphocholine analogs with specificity for gliomas. Their efforts are timely in that the mounting literature in support of glioma extent of resection necessitates new paradigms, including fluorescent-guided surgery, to maximize cytoreduction. We look forward to more work from this group further validating this fluorophore biomarker and exploring its utility in both diagnostic and therapeutic paradigms.

Nader Sanai
Phoenix, Arizona

This is an interesting article examining the use of alkylphosphocholine analogs as a potential aid to fluorescence-guided glioma surgery. The major limitation of this report is the xenograft nature of the model used for these studies. I also am not convinced that the comparison of these new markers with the more established fluorescent-based surgical aids (such as 5-aminolevulinic acid) is reasonable on the basis of the data presented in this report. Although these compounds might prove useful in the future, further work is required.

Randy Jensen
Salt Lake City, Utah

A video abstract discussion by Drs Kuo and Weichert accompanies this article. Please visit http://bit.ly/1GxvFOx to view this video.